Article

Ranging Correlated Motion (1.5 nm) of Two Coaxially Arranged Rotors Mediated by Helix Inversion of a Supramolecular Transmitter

Shuichi Hiraoka, Erika Okuno, Takaaki Tanaka, Motoo Shiro, and Mitsuhiko Shionoya

J. Am. Chem. Soc., **2008**, 130 (28), 9089-9098 • DOI: 10.1021/ja8014583 • Publication Date (Web): 18 June 2008

J|A|C|S
ARTICLES

Published on Web 06/18/2008

Ranging Correlated Motion (1.5 nm) of Two Coaxially Arranged Rotors Mediated by Helix Inversion of a Supramolecular Transmitter

Shuichi Hiraoka,*[,†,‡] Erika Okuno,[†] Takaaki Tanaka,[†] Motoo Shiro,[§] and Mitsuhiko Shionoya*[,†]

Department of Chemistry, Graduate School of Science, The University of Tokyo, 7-3-1 Hongo, Bunkyo-ku, Tokyo 113-0033, Japan, Precursory Research for Embryonic Science and Technology (PRESTO), Japan Science Technology Agency, 4-1-8 Honcho, Kawaguchi, Saitama 332-0012, Japan, and Rigaku Corporation, 3-9-12 Matsubaracho, Akishima, Tokyo 196-8666, Japan

Received February 27, 2008; E-mail: shionoya@chem.s.u-tokyo.ac.jp; hiraoka@chem.s.u-tokyo.ac.jp

Ⓦ **This paper contains enhanced objects available on the Internet at http://pubs.acs.org/jacs.**

Abstract: For a long-range transmission of motion between two movable parts apart from each other, transmitters that can precisely correlate these two motions should be properly incorporated into the system. However, such a motional relay is yet to be realized in artificial systems because of the lack of reliable methodologies for arranging a discrete number of motional parts. Herein, we report a correlated motion of two rotor molecules, which are coaxially arranged at a distance of 1.5 nm, through either Ag^{+}- or Hg^{2+}-assembled helical transmitters, leading to different frequencies of synchronized motion. A helix inversion in the transmitter was proven to strongly correlate the motions of both terminals. The X-ray analysis of the entity determined a quadruple-decker nonanuclear structure of the metal complex comprising two terminal rotor-like ligands closely attached to a central transmitter moiety. ^{1}H NMR analysis fully demonstrated the synchronized motion of the two rotors coaxially stacked and connected through the transmitter. Since the transmitter is composed of simple helical repeating units, the principle of helix inversion would be an efficient and widely applicable strategy for the long-range transmission of molecular motion.

Introduction

In a macroscopic machine the rotation of a motor turns a terminal actuator through intermediate shafts and gears. Essentially, two (rotational) motions, on either side of a simple mechanical device, are correlated by an in-between part called a "transmitter" herein. Likewise, elaborate transmission or transformation of molecular motions is essential for developing simple molecular motions to more sophisticated mechanical actions used in artificial molecular machine systems. In early studies on molecular machines,[1] the use of steric interactions between two covalently linked contiguous gearlike parts is a classical but rational strategy to join these two motional parts. The first report on the correlated motion between two artificial gear molecules was back in the 1970s,[2] in which adjacent benzene rings interact with each other within the molecules through steric interactions. Since then, a large number of two-gear systems, that can convert the rate of rotation using a different number of tooth or the direction of rotation axis, have been realized by simple organic molecules,[3–5] metal-coordination compounds,[6–10] and hybridized circular DNA strands.[11] Beyond two-gear systems in which two movable parts interact directly with each other (Figure 1A,B), the multigear systems that were reported, however, are attained in a circular array of small aromatic rings attached to a benzene ring[12] or linear oligomers with rotation of aromatic rings along carbon−carbon single bonds of a main chain.[13,14] In our view, it is intrinsically impossible to transmit motions at a long-range in the former

[†] The University of Tokyo.
[‡] Japan Science Technology Agency.
[§] Rigaku Corporation.

(1) (a) Balzani, V.; Venturi, M.; Credi, A. *Molecular Devices and Machines—A Journey into the Nano World*; Wiley-VCH: Weinheim, Germany, 2003. (b) Feringa, B. L. *J. Org. Chem.* **2007**, *72*, 6635. (c) Kay, E. R.; Leigh, D. A.; Zerbetto, F. *Angew. Chem., Int. Ed.* **2006**, *46*, 72. (d) Sauvage, J.-P. *Chem. Commun.* **2005**, 1507. (e) Saha, S.; Stoddart, J. F. *Chem. Soc. Rev.* **2007**, *36*, 77.
(2) Gust, D.; Mislow, K. *J. Am. Chem. Soc.* **1973**, *95*, 1535.
(3) Iwamura, H.; Mislow, K. *Acc. Chem. Res.* **1988**, *21*, 175.
(4) Yamamoto, G.; Ōki, M. *J. Org. Chem.* **1983**, *48*, 1233.
(5) Kottas, G. S.; Clarke, L. I.; Horinek, D.; Michl, J. *Chem. Rev.* **2005**, *105*, 1281.
(6) Brydges, S.; Harrington, L. E.; McGlinchey, M. J. *Coord. Chem. Rev.* **2002**, *233−234*, 75.
(7) Stevens, A. M.; Richards, C. J. *Tetrahedron Lett.* **1997**, *38*, 7805.
(8) Romeo, R.; Carnabuci, S.; Fenech, L.; Plutino, M. R.; Albinati, A. *Angew. Chem., Int. Ed.* **2006**, *45*, 4494.
(9) Bulo, R. E.; Allaart, F.; Ehlers, A. W.; de Kanter, F. J. J.; Schakel, M.; Luts, M.; Spek, A. L.; Lammertsma, K. *J. Am. Chem. Soc.* **2006**, *128*, 12169.
(10) Carella, A.; Jaud, J.; Rapenne, G.; Launary, J. P. *Chem. Commun.* **2003**, 2434.
(11) Tian, Y.; Mao, C. *J. Am. Chem. Soc.* **2004**, *126*, 11410.
(12) Gust, D.; Patton, A. *J. Am. Chem. Soc.* **1978**, *100*, 8175.
(13) Lindner, A. B.; Grynszpan, F.; Biali, S. E. *J. Org. Chem.* **1993**, *58*, 6662.
(14) Coluccini, C.; Grilli, S.; Lunazzi, L.; Mazzanti, A. *J. Org. Chem.* **2003**, *68*, 7266.

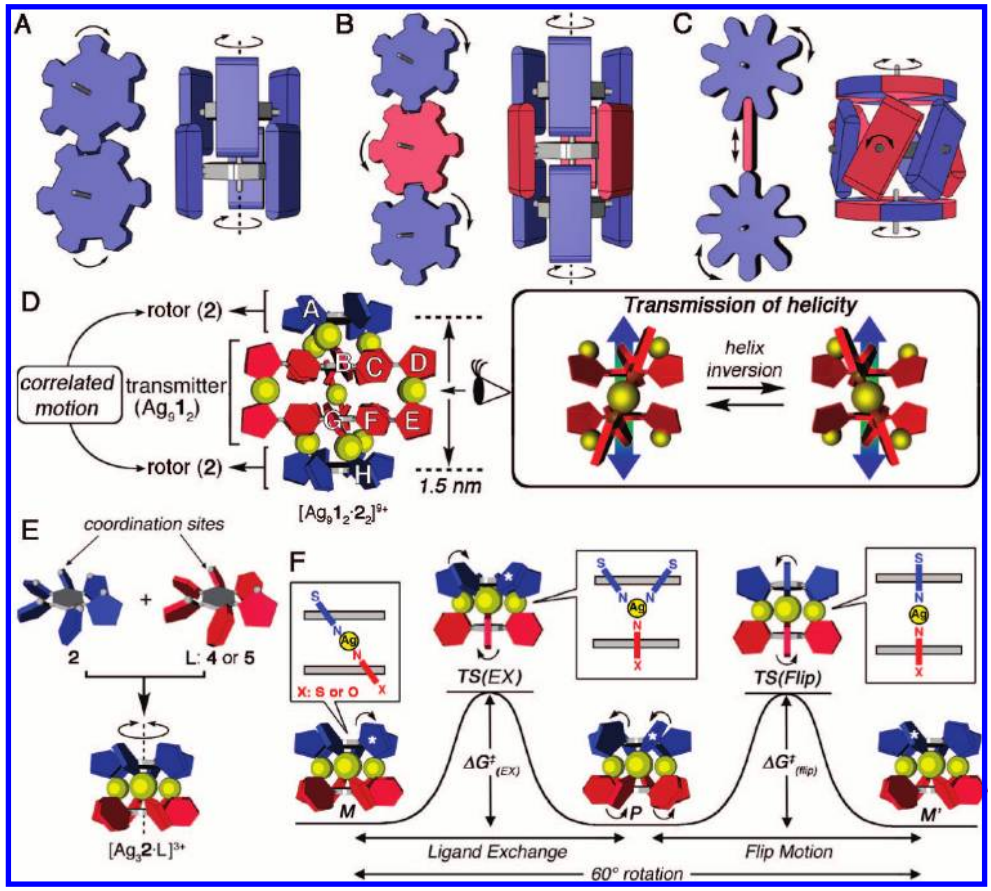

Figure 1. (A−C) Schematic representation of correlated motions between two rotational parts. (A) Two gears with parallel rotation axes (left) and a coaxis (right). The motions of two gears are correlated by their direct steric interaction. (B) A rotational transmitting system: the motions of two gears (blue) are correlated through a rotational motion of a central transmitter (red). (C) Outline drawing of an oscillation transmitting system: the motions on both sides are mediated by oscillating motions of a central transmitter. (Left) A linear oscillating transmitter. (right) A circular oscillating transmitter, in which two parts (red and blue) are alternately arranged in both the rotor and the transmitter and have a higher affinity for that in the same color. The rotation of the rotor on one side induces the circular oscillating motion of blades in the transmitter, and thereby the rotor on the other side is allowed to rotate cooperatively. (D) (Left) A design concept of a molecular rotor−transmitter−rotor device, $[Ag_9\mathbf{1}_2\cdot\mathbf{2}_2]^{9+}$, composed of a transmitter ($[Ag_9\mathbf{1}_2]^{9+}$) and two rotors (**2**). The rotation on one side propagates to the other side on a steric demand between the rings both in the rotors and transmitter, for example, rings **A** to **H**. (Right) The helix inversion of transmitter $[Ag_9\mathbf{1}_2]^{9+}$ mediates the motions of two rotors, **2** (movie 1). (E) A molecular ball bearing consisting of a hexa-monodentate ligand **2**, a tris-monodentate ligand **L** (**4** or **5**), and three Ag^+ ions. The ligand **L** arranges the three Ag^+ ions in triangle, while six ligand rings in **2** participate in the intramolecular ligand exchange that causes the relative rotation. (F) A proposed mechanism of a relative rotation of the two rotors in the molecular ball bearings, $[Ag_3\mathbf{2}\cdot\mathbf{L}]^{3+}$. A 60° relative rotation consists of a ligand exchange and a flip motion (movie 2). The ligand exchange takes place on three Ag^+ ions simultaneously, that is, every second ligand ring of **2** coordinating to Ag^+ exchanges with the neighboring coordinatively free ligand rings accompanying the helix inversion of the complex. The flip motion also accompanies the helix inversion retaining the N−Ag−N bonds.

Ⓦ movie 1, showing the helix inversion of transmitter $[Ag_9\mathbf{1}_2]^{9+}$ mediating the motions of two rotors, **2**, is available.

Ⓦ movie 2, showing a 60° relative rotation consisting of a ligand exchange and a flip motion, is available.

case, and even in the latter case it is rather difficult to precisely control the transmission. Thus, a new synthetic strategy to allow long-range transmission of motions through a well-designed transmitter molecule that can precisely synchronize more than two motions, has been long-awaited.[15]

Molecular Design of Rotor−Transmitter−Rotors (RTRs). Recently, we first reported a supramolecular rotational device, $[Ag_3\mathbf{2}\cdot\mathbf{4}]^{3+}$ complex, which behaves like a *ball bearing* (Figure 1E).[16,17] In this molecule, the random processes of a ligand exchange ($M \leftrightarrow P$ in Figure 1F) and a flip motion ($P \leftrightarrow M'$ in Figure 1F) allow the two rotor parts, **2** and **4**, to rotate relatively to each other (rotation in either direction, back and forth motion, and their combination). Both motions take place between the *P* and *M* helical enantiomers of $[Ag_3\mathbf{2}\cdot\mathbf{4}]^{3+}$ (Figure 1F and movie 2),[18] and the motions of the rings in the two rotors are precisely synchronized with each other through their helix inversion. In this view, a transmitter that can mediate the helix inversion was expected to correlate the two rotational motions. We have then newly designed a supramolecular transmitter that can correlate two rotational motions through an oscillating helix inversion, as shown in Figure 1C (right). The transmitter has a metal-assembled helical structure, $[Ag_6M_3\mathbf{1}_2]^{(6+3n)+}$ (M^{n+}: Ag^+ or Hg^{2+}), and the helix inversion between two helical optical isomers, *P* and *M*, can correlate the motions of two disk-shaped rotor molecules, **2**. The two rotors are ca. 1.5 nm apart and coaxially connected with the central transmitter through metal

(15) Muraoka, T.; Kinbara, K.; Aida, T. *Nature* **2006**, *440*, 512.
(16) Hiraoka, S.; Shiro, M.; Shionoya, M. *J. Am. Chem. Soc.* **2004**, *126*, 1214.
(17) Hiraoka, S.; Hirata, K.; Shionoya, M. *Angew. Chem., Int. Ed.* **2004**, *43*, 3814.
(18) Hiraoka, S.; Harano, K.; Tanaka, T.; Shiro, M.; Shionoya, M. *Angew. Chem., Int. Ed.* **2003**, *42*, 5182.

Chart 1. Ligands **1**−**5** Used in This Study[a]

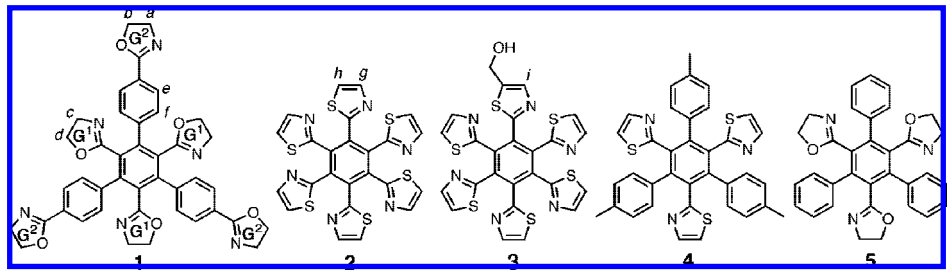

[a] The letters denote the ^{1}H NMR assignments in Figure 2.

coordination (Figure 1D). The ligand **1** has a central benzene ring carrying alternating oxazolinyl and oxazolinylphenyl groups on two concentric circles. That is, three oxazoline ligands ($\mathbf{G^1}$) are placed on the inner circle and the other three oxazoline ligands ($\mathbf{G^2}$) on the outer circle. It was thereby expected that the three ligands $\mathbf{G^1}$ of **1** act as a partner of a terminal rotor **2** through Ag^+-mediated self-assembly, while the other three ligands $\mathbf{G^2}$ of **1** serve as a joint within the metal-mediated transmitter. From a molecular modeling study, it was most likely that in the resulting molecular rotor−transmitter–rotor (RTR), $[Ag_6M_3\mathbf{1}_2\cdot\mathbf{2}_2]^{(6+3n)+}$, four disk-shaped ligands are coaxially stacked with the aid of nine metal ions, and that both the transmitter and rotors in the RTR have a helical structure. Thus, the propagation of a helicity from one side of the rotor **2** to the other side (ring **A** to ring **H** in Figure 1D left) should be mediated by the synchronous helix inversion that takes place in the rotors and the transmitter. The helix inversion of on one side of the rotor **2** (ring **A**) as a result of the ligand exchange or the flip motion brings about the conversion of the helicity of **1** (rings **B** and **C**) in the transmitter through Ag(I)−N coordination bonds between the rotor and the transmitter. And then, the outer oxazoline rings (ring **D**) in **1** rotate to switch the helicity of the other side of **1** (ring **E**) through Ag(I)−N coordination bonds in the transmitter. As the result, the helicity of the other side of the rotor (ring **H**) connected to the transmitter is simultaneously converted. Since the two disk-shaped ligands **1** are closely placed, it is probable that the propagation of the helicity should occur face-to-face through a direct contact between the rings (ring **B** to **G** and **C** to **F**). Both the propagation pathways should allow a synchronous motion with the two terminal rotors, **2**, through the helix inversion of the central transmitter $[Ag_6M_3\mathbf{1}_2]^{(6+3n)+}$ (movie 1).

Results and Discussion

Syntheses of Disk-Shaped Ligands. The disk-shaped multimonodentate ligands **1**−**5** shown in Chart 1 were synthesized by the cobalt-catalyzed trimerization of alkyne derivatives. The synthetic procedure for disk-shaped ligands **1**,[19] **2**,[16] and **4**[18] was previously reported. Disk-shaped hexa-monodentate ligands, **3** and **5**, were synthesized according to Scheme S1 (see the Supporting Information).

Formation of Molecular RTRs. Molecular RTRs, $[Ag_6M_3\mathbf{1}_2\cdot\mathbf{X}_2]^{(6+3n)+}$ (X: **2** or **3**; M^{n+}: Ag^+ or Hg^{2+}), were quantitatively formed by simply mixing a set of components in CD_3OD. The resulting entities were fully characterized in solution by ^{1}H NMR spectroscopy and electrospray ionization time-of-flight (ESI-TOF) mass spectrometry. For example, a nonanuclear $[Ag_9\mathbf{1}_2\cdot\mathbf{2}_2]^{9+}$ complex was immediately formed from **1**, **2**, and AgOTf (OTf:CF_3SO_3) in a 2:2:9 ratio in CD_3OD at room temperature. The ^{1}H NMR spectrum of $[Ag_9\mathbf{1}_2\cdot\mathbf{2}_2]^{9+}$ at 313 K showed well-resolved, simple resonances, suggesting the quantitative formation of a discrete structure with a high symmetry (Figure 2). It is notable that the signals for protons *e* and *f* of **1** appeared as four resonances, indicating that two faces of the disk-shaped ligand **1** are nonequivalent to each other as a result of the formation of the $[Ag_9\mathbf{1}_2\cdot\mathbf{2}_2]^{9+}$ complex.[16] Its ESI-TOF mass spectrum showed two prominent signals at m/z = 2304.5 and 1487.1, which are assignable to $[Ag_9\mathbf{1}_2\cdot\mathbf{2}_2\cdot(OTf)_7]^{2+}$ and $[Ag_9\mathbf{1}_2\cdot\mathbf{2}_2\cdot(OTf)_6]^{3+}$, respectively (Figure S3 in the Supporting Information). We thereby concluded that the $[Ag_9\mathbf{1}_2\cdot\mathbf{2}_2]^{9+}$ complex is exclusively formed in solution.

Single-Crystal X-Ray Analysis. A single-crystal suitable for X-ray diffraction study was obtained from a saturated CH_3OH solution of $Ag_9\mathbf{1}_2\cdot\mathbf{2}_2\cdot(OTf)_9$. The crystal structure contained a nonanuclear $[Ag_9\mathbf{1}_2\cdot\mathbf{2}_2]^{9+}$ cation together with nine uncoordinated TfO^- anions (Figure 3A−C). Its quadruple-decker structure can be best described as an assembly of two outer (**2**) and two inner (**1**) disk-shaped ligands stacked on top of each other with the aid of nine Ag^+ ions. The total length of the molecule along the rotation axis is ca. 21 Å and the two terminal rotors (**2**) are 1.5 nm apart. Each Ag^+ ion is linear two-coordinate, and therefore every second thiazole nitrogen atom in **2** is coordinatively free. All the ligand ring planes of the four disks are not perpendicular to the central benzene ring planes, resulting in the formation of a helical structure (*P* or *M* form). A set of enantiomers is included in a unit cell to form a racemate. The oxazoline and phenylene rings attached directly to the central benzene rings in **1** ($\mathbf{G^1}$) and all the thiazolyl rings in **2** tilt toward the same direction by ca. 30° from the rotation axis. On the other hand, the outer three oxazoline rings ($\mathbf{G^2}$) in **1** tilt in the opposite helical sense by ca. 10°. This observation indicates the structural interlocking of the four ligands in the entity. As shown in the molecular packing of $[Ag_9\mathbf{1}_2\cdot\mathbf{2}_2]^{9+}$ in the crystal (Figure 3C), the cationic parts, $[Ag_9\mathbf{1}_2\cdot\mathbf{2}_2]^{9+}$, are completely separated from each other, and their rotational axes are arranged in parallel rows.

Relative Rotation of Rotors in the Molecular RTRs. Relatively free rotation of the two rotors in the RTRs was demonstrated by examining the symmetry of the complexes, $[Ag_6M_3\mathbf{1}_2\cdot\mathbf{3}_2]^{(6+3n)+}$ (M^{n+}: Ag^+ or Hg^{2+}), including two hexa-monodentate ligands **3** with C_{2v} symmetry. If the rate of the rotation is faster than the NMR time scale, the proton signals for **1** in the transmitter should appear in the same way as their original ligand **2** with C_3 symmetry. That is, the oxazolinyl proton signals *a*−*d* of **1**, for example, should be observed as one set. The proton signals of **3** in the $[Ag_9\mathbf{1}_2\cdot\mathbf{3}_2]^{9+}$ complex, on the other hand, are not informative enough to describe the

(19) Hiraoka, S.; Tanaka, T.; Shionoya, M. *J. Am. Chem. Soc.* **2006**, *128*, 13038.

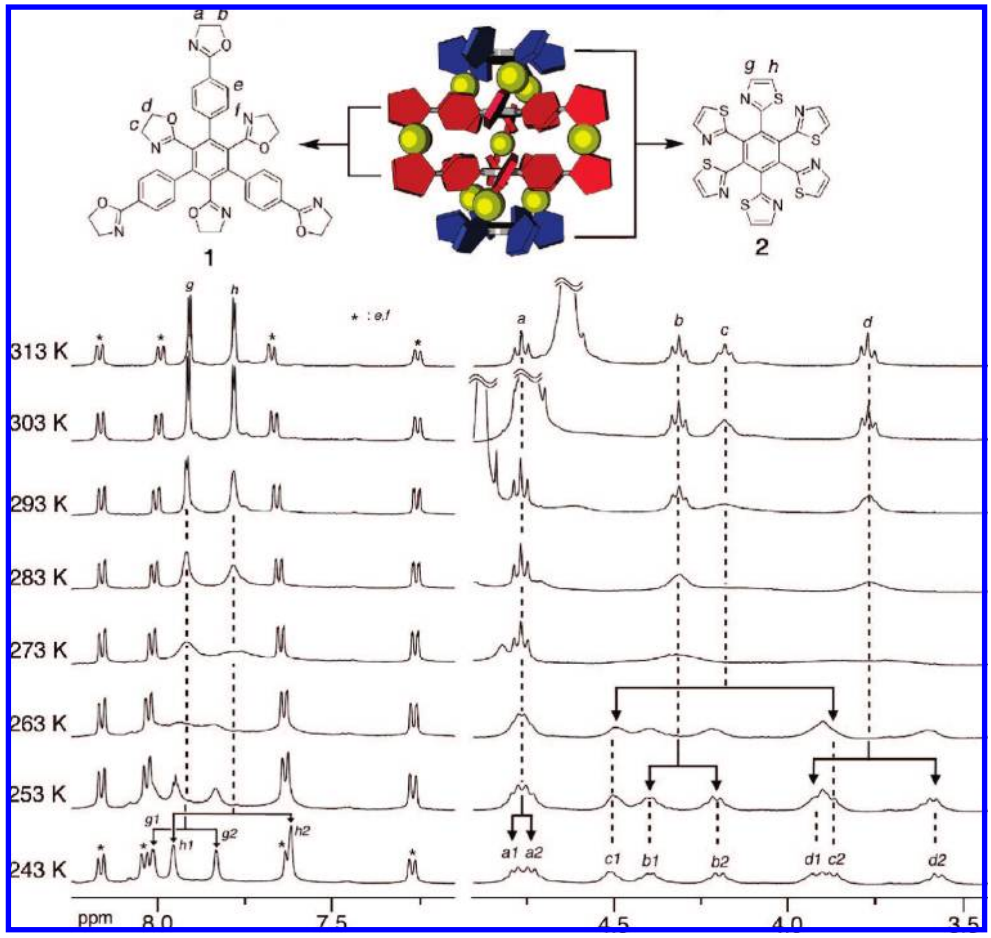

Figure 2. Partial VT ^{1}H NMR spectra (500 MHz, CD_3OD) of a molecular rotor−transmitter−rotor, $Ag_9\mathbf{1}_2\cdot\mathbf{2}_2\cdot(OTf)_9$. $[Ag_9\mathbf{1}_2\cdot\mathbf{2}_2\cdot(OTf)_9] = 3.7$ mM.

rotation in detail, because these signals should not show any changes even when the rate of the flip motion becomes slower than the NMR time scale on the assumption that the energy barrier of the flip motion, $\Delta G^{\ddagger}_{flip}$, is greater than that of the ligand exchange, $\Delta G^{\ddagger}_{ex}$. The detailed comparative investigation of the energy profile of these two motions in the molecular ball bearings with ligand **3** will be reported elsewhere. The quantitative formation of $[Ag_9\mathbf{1}_2\cdot\mathbf{3}_2]^{9+}$ was demonstrated by ^{1}H NMR titration studies (Figure S2) and ESI-TOF mass measurements (Figure S4). The ^{1}H NMR spectrum of $[Ag_9\mathbf{1}_2\cdot\mathbf{3}_2]^{9+}$ at 303 K showed two inequivalent oxazoline rings assignable to the inner and outer rings, indicating the rapid rotation of the rotors with C_{2v} symmetry on the NMR time scale (Figure 4). Upon cooling down to 243 K, the signals for **1** and **3** became broadened and more complicated (Figure S7). This is well explained by the fact that the rate of the rotation becomes slower than the NMR time scale around this temperature.

Motional Correlation. As both the ligand exchange and the flip motion take place with the helix inversion of the structure, the analysis of the helix inversion is the most useful way to assess the motional correlation in $[Ag_9\mathbf{1}_2\cdot\mathbf{2}_2]^{9+}$. In other words, the rate of helix inversion in the rotors **2** can be determined from the motion of the inner oxazoline rings ($\mathbf{G^1}$), and then compared with the rate of helix inversion of the outer oxazoline rings of **1** ($\mathbf{G^2}$) in the transmitter. If the motion of the two terminal rotors **2** are synchronized with each other, the rates of helix inversion (k_{helix}) of the inner and outer oxazoline rings in **1** should be identical and prove that the helix inversions of both the rotors and the transmitter take place at the same frequency. In this case, the proton signals for oxazoline rings, *a*−*d*, are good indicators to analyze the helix inversion of both the inner and outer rings, because two geminal protons in the oxazoline rings are inequivalent, provided that the helix inversion is rather slow compared with the NMR time scale (Figure 5D). However, in addition to the helix inversion, the chemical exchange between these geminal protons would take place due to the ring flip of oxazoline rings with twisted-boat conformation (Figure 5A). To evaluate the rate of the ring flip, variable-temperature (VT) ^{1}H NMR measurements of both free ligand **1** and sandwich-shaped $[Ag_6\mathbf{1}_2]^{6+}$ complex[19] (Figure 5C), in which six Ag^+ ions are placed between the two ligands, were performed. The oxazolinyl protons in both **1** and $[Ag_6\mathbf{1}_2]^{6+}$ showed almost no changes but became slightly broadened at temperature as low as 193 K, indicating that the ring flip is so fast on the NMR time scale or that oxazoline rings are flat (as shown in the nearly planar conformation of oxazoline rings in the crystal structure of $[Ag_9\mathbf{1}_2\cdot\mathbf{2}_2]^{9+}$). Therefore, the ring flip is negligible in the present VT NMR analysis of the $[Ag_9\mathbf{1}_2\cdot\mathbf{2}_2]^{9+}$ complex. As the temperature of solutions of $[Ag_9\mathbf{1}_2\cdot\mathbf{2}_2]^{9+}$ in CD_3OD was lowered, the oxazolinyl proton signals, *a*−*d*, were divided into two sets arising from slower helix inversion compared with the NMR time scale (Figure 6A). The line-shape analysis of the oxazolinyl proton signals clarified that the helix inversion of the inner and outer oxazoline rings takes place at almost the same rate at temperatures ranging from 293 to 253 K (Figure 6B). This result demonstrates that all the rings in the rotors and the transmitter bring about the helix inversion at the same frequency, that is, a synchronous motion

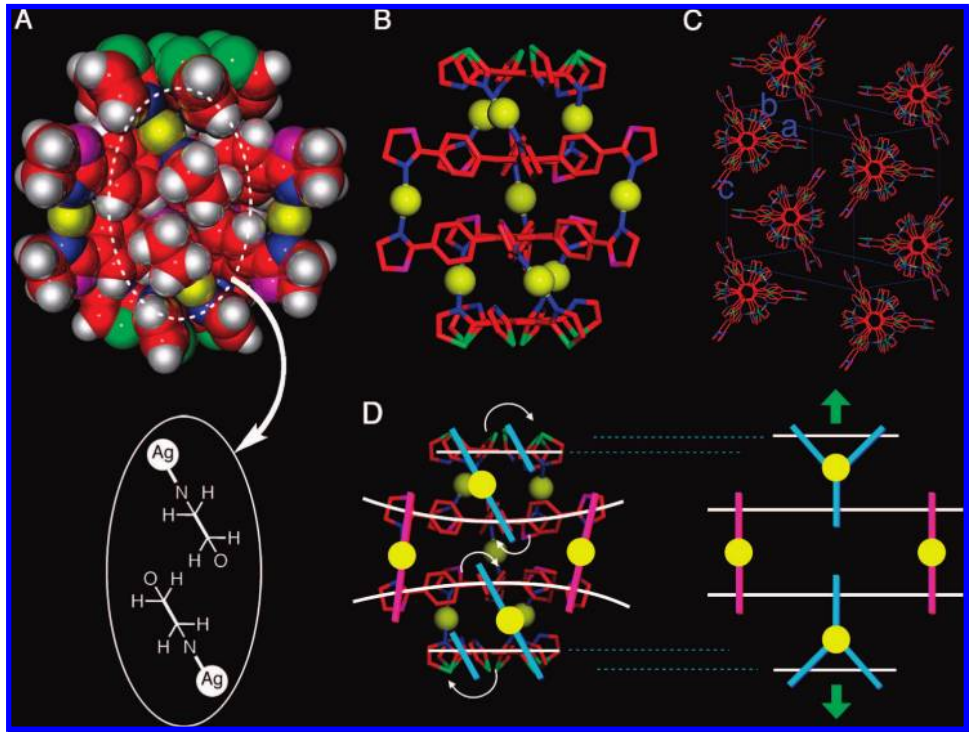

Figure 3. Crystal structure of the $Ag_9\mathbf{1}_2\cdot\mathbf{2}_2\cdot(OTf)_9$ complex. (A) A space filling model. (B) A cylinder model. Hydrogen atoms are omitted for clarity. Color labels: red, carbon; yellow, silver, blue, nitrogen; purple, oxygen; green, sulfur. (C) A packing diagram of $[Ag_9\mathbf{1}_2\cdot\mathbf{2}_2]^{9+}$ viewed from a rotation axis of the complex. Hydrogen atoms and counteranions are omitted for clarity. (D) Schematic depiction of the proposed ground and transition geometries of the ligand exchange processes taking place in the $[Ag_9\mathbf{1}_2\cdot\mathbf{2}_2]^{9+}$ complex.

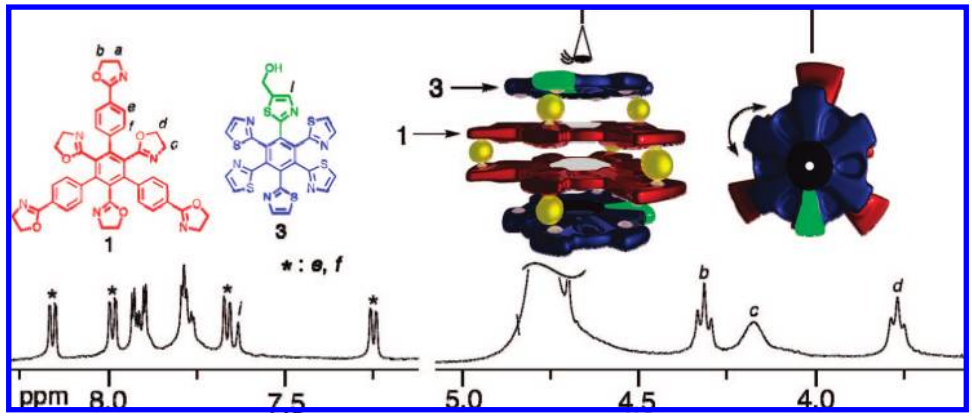

Figure 4. Partial VT ^{1}H NMR spectrum (500 MHz, CD_3OD) of $Ag_9\mathbf{1}_2\cdot\mathbf{3}_2\cdot(OTf)_9$ ($[Ag_9\mathbf{1}_2\cdot\mathbf{3}_2\cdot(OTf)_9] = 4.0$ mM, 303 K.

of the two terminal rotors **2** mediated by the helix inversion of the central transmitter. The kinetic parameters for the helix inversion were determined to be $\Delta H^{\ddagger}_{helix} = 77$ kJ mol^{-1} and $\Delta S^{\ddagger}_{helix} = 38$ J mol^{-1} K^{-1}. It should be noted that a large, positive entropy change suggests the cooperativity of the motion. Considering that the helix inversion is a combination of the ligand exchange and the flip motion, we shall discuss these parameters along with the ligand exchange and the flip motion in the following sections.

Intramolecular Multipoint Ligand Exchanges in an RTR. As expected from the interlocked structure of $[Ag_9\mathbf{1}_2\cdot\mathbf{2}_2]^{9+}$, as evidenced by molecular modeling and the crystal structure, the rotation of the terminal rotors **2** with a combination of ligand exchange and the flip motion should be strongly affected by the supramolecular transmitter. The intramolecular three-point ligand exchange arising in the rotors of $[Ag_9\mathbf{1}_2\cdot\mathbf{2}_2]^{9+}$ was then studied in detail by VT ^{1}H NMR spectroscopy. As the temperature of the CD_3OD solution of $[Ag_9\mathbf{1}_2\cdot\mathbf{2}_2]^{9+}$ was lowered, the proton signals *g* and *h* of **2** became broadened around 263 K and finally divided into two sets at 243 K (Figure 2). The kinetic parameters for the ligand exchange, $\Delta H^{\ddagger}_{ex}$ and $\Delta S^{\ddagger}_{ex}$, were determined to be 77.7 kJ mol^{-1} and 46.1 J mol^{-1} K^{-1}, respectively (Table 1). The rate constant for $[Ag_9\mathbf{1}_2\cdot\mathbf{2}_2]^{9+}$ at 298 K, 1×10^4 s^{-1}, is about twenty times smaller than that of a monomeric molecular ball bearing, $[Ag_3\mathbf{2}\cdot\mathbf{5}]^{3+}$, and the enthalpy change ($\Delta H^{\ddagger}_{ex}$) was found greater with $[Ag_9\mathbf{1}_2\cdot\mathbf{2}_2]^{9+}$. It is apparent that these significant differences come from the supramolecular transmitter connecting the terminal rotors. The larger $\Delta H^{\ddagger}_{ex}$ for $[Ag_9\mathbf{1}_2\cdot\mathbf{2}_2]^{9+}$ should arise from the steric interactions of rings between two ligands **1** in the transmitter. Furthermore, the entropy changes ($\Delta S^{\ddagger}_{ex}$) showed a significant difference as shown in a large positive $\Delta S^{\ddagger}_{ex}$ value, 46.1 J mol^{-1} K^{-1}, for RTR, $[Ag_9\mathbf{1}_2\cdot\mathbf{2}_2]^{9+}$, and a negative $\Delta S^{\ddagger}_{ex}$ value, -9.2 J mol^{-1} K^{-1}, for molecular ball bearing, $[Ag_3\mathbf{2}\cdot\mathbf{5}]^{3+}$. Three

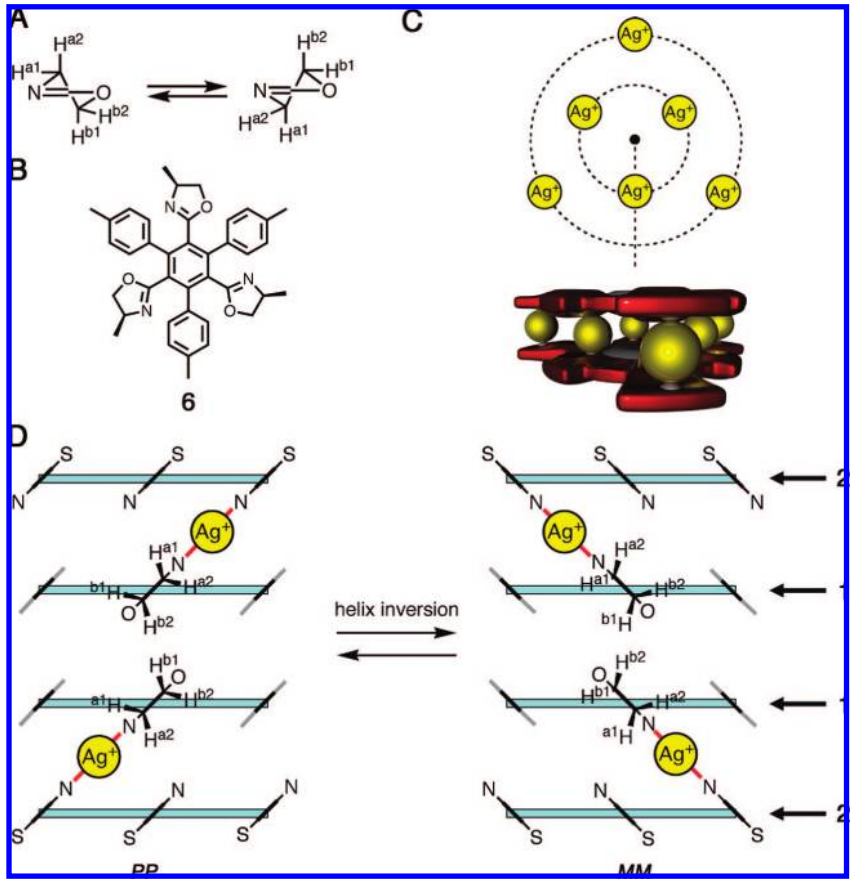

Figure 5. (A) Ring flip of an oxazoline ring between two twisted-boat conformations. (B) Chemical structure of asymmetric tris-monodentate ligand **6**. VT NMR spectra of $[Ag_3\mathbf{2}\cdot\mathbf{6}]^{3+}$ were reported in ref 17. (C) Schematic representation of $[Ag_6\mathbf{1}_2]^{6+}$ complex. The synthesis and structural characterization of the complex were reported in ref 19. (D) Schematic representation of the helix inversion in $[Ag_6M_3\mathbf{1}_2\cdot\mathbf{2}_2]^{(3n+6)+}$ complexes ($M^{n+} = Ag^+$ or Hg^{2+}). *PP* and *MM* denote screw senses of the two molecular ball bearing moieties ($[Ag_3\mathbf{1}\cdot\mathbf{2}]^{3+}$) in their structures.

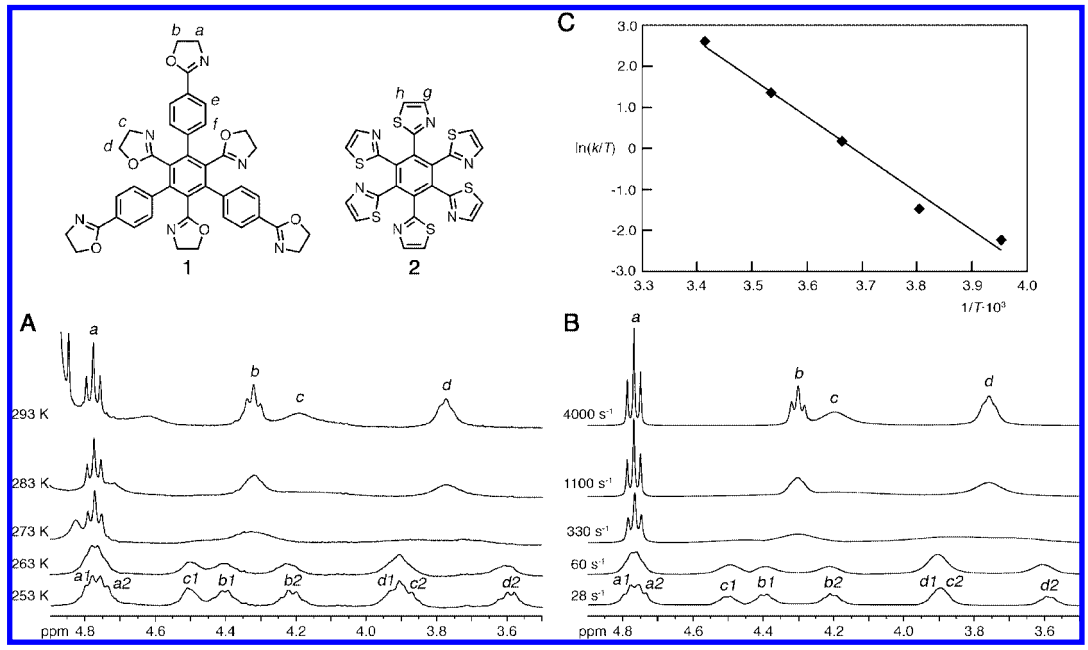

Figure 6. (A) Partial VT ^{1}H NMR spectra of $[Ag_9\mathbf{1}_2\cdot\mathbf{2}_2]^{9+}$ complex (500 MHz, CD_3OD, [**1**] = [**2**] = 3.7 mM). (B) Simulated spectra of H^a, H^b, H^c, and H^d protons for various exchange rates. (C) Eyring plots.

additional Ag−N bonds in the plausible three-coordinate Ag^+ centers in the transition state (TS_{ex}) of the intramolecular ligand exchange should be the primary reason for the negative $\Delta S^{\ddagger}_{ex}$ observed for $[Ag_3\mathbf{2}\cdot\mathbf{5}]^{3+}$.[16] Although a negative $\Delta S^{\ddagger}_{ex}$ was similarly expected owing to the six additional Ag−N bonds formed in the transition state of $[Ag_9\mathbf{1}_2\cdot\mathbf{2}_2]^{9+}$; in fact, a large

Table 1. Kinetic Parameters of Intramolecular Ligand Exchange for Molecular Ball Bearing and Rotor−Transmitter−Rotor Devices[a]

complex	$\Delta H^{\ddagger}$ (kJ mol^{-1})	$\Delta S^{\ddagger}$ (J mol^{-1} K^{-1})	$\Delta G^{\ddagger}$ (kJ mol^{-1})	k at 298 K (s^{-1})
$[Ag_3\mathbf{2}\cdot\mathbf{5}]^{3+}$	51.7	−9.2	54.4	2×10^5
$[Ag_9\mathbf{1}_2\cdot\mathbf{2}_2]^{9+}$	77.7	46.1	63.9	1×10^4
$[Ag_6Hg_3\mathbf{1}_2\cdot\mathbf{2}_2]^{12+}$	67.9	5.3	66.3	4×10^3

[a] Determined by the line shape analysis of the chemical exchange of thiazolyl protons of **2**.

positive $\Delta S^{\ddagger}_{ex}$ value was obtained. This is probably because two ligands **1** in the transmitter are bent in the ground-state so that the motion of the rings in $[Ag_9\mathbf{1}_2\cdot\mathbf{2}_2]^{9+}$ may be highly restrained (Figure 3D), as was observed in the crystal structure and judged from the molecular modeling. On the other hand, the structure of $[Ag_9\mathbf{1}_2\cdot\mathbf{2}_2]^{9+}$ in the transition state of the ligand exchange process is considered stretched along the rotation axis so that the rings can move without hindrance. Thus, it appears that the large positive $\Delta S^{\ddagger}$ value for $[Ag_9\mathbf{1}_2\cdot\mathbf{2}_2]^{9+}$ arises from the partially compacted structure around the metal centers of rotors in the ground state. These results indicate that the helix inversion of the transmitter would strongly affect the rotational motions of the two terminal rotors.

Flip Motion. In the flip motion, which is the other basic motion in the rotation mechanism (Figure 1F), the rate of flip motion (k_{flip}) in $[Ag_9\mathbf{1}_2\cdot\mathbf{2}_2]^{9+}$ should become considerably slower than a molecular ball bearing, $[Ag_3\mathbf{2}\cdot\mathbf{5}]^{3+}$, as expected from its slower ligand exchange. The flip motion is accompanied by a helix inversion between two enantiomers with retention of all the Ag−N bonds during the process. In general, it is hard to analyze the flip motion of an achiral molecular ball bearing. Indeed, to assess the flip motion, diastereomeric complexes having chiral tris-monodentate ligands[17] or counteranions[18] are needed. Since both the ligand exchange and the flip motion accompany a helix inversion, the k_{helix} should be the summation of the rate constants of both motions (k_{ex} and k_{flip}), that is, $k_{helix} = k_{ex} + k_{flip}$. Therefore, k_{flip} can be estimated from k_{ex} and k_{helix} which were determined experimentally by analyzing the chemical exchanges of the thiazolyl protons of **2** and oxazolinyl protons of **1**, respectively. Thus, k_{helix} at every temperature should be greater than k_{ex}. However, the line shape analysis of these proton signals at various temperatures indicates slower rate constants of the helix inversion. This result contradicts the above-mentioned considerations. The slower rate constants of the chemical exchange of the oxazolinyl protons could be attributed to their relatively broadened signals. This is probably due to the temperature-dependent conformational changes of the oxazoline rings. These factors should affect evenly all the oxazolinyl protons so that one can compare the chemical exchange of these protons. The VT NMR measurement of $[Ag_9\mathbf{2}_2\cdot\mathbf{3}_2]^{9+}$ containing **3** with C_{2v} symmetry clearly showed that the rotation of the terminal rotors is fast on the NMR time scale at 303 K, indicating that the flip motion is also fast on the NMR time scale at the temperature. In light of these results, we conclude that the flip motion is slower than the ligand exchange but still fast on the NMR time scale at 303 K. Thus, k_{flip} would reach at least 1000 s^{-1} at 298 K. The relatively slower flip motion in $[Ag_9\mathbf{1}_2\cdot\mathbf{2}_2]^{9+}$ is contradistinctive. In the case of a monomeric ball bearing, the flip motion is much faster than the ligand exchange. For example, any diastereotopic proton signals were not observed for $[Ag_3\mathbf{2}\cdot\mathbf{6}]^{3+}$ with asymmetric tris-monodentate ligand **6** (Figure 5B) even at 193 K, whereas two sets of thiazolyl signals of **2** were observed, indicating that the flip motion is faster than the ligand exchange.[17] Thus, the energy barrier of the flip motion in molecular RTR, $[Ag_9\mathbf{1}_2\cdot\mathbf{2}_2]^{9+}$, is considerably heightened and becomes larger than that of the ligand exchange. This is probably because the stretched structure in the transition state of the flip motion, in which all the rings attached to the central benzene rings are parallel to the rotation axis, gets rather unstable compared with that of the intramolecular ligand exchange.

$[Ag_6Hg_3\mathbf{1}_2]^{12+}$ Transmitter. As described above, the connection of the two terminal rotors by a supramolecular transmitter $[Ag_9\mathbf{1}_2]^{9+}$ resulted in an intramolecular motional correlation between them at a distance of 1.5 nm. The changes in the size and the charge number of metal ions in the $[Ag_6M_3\mathbf{1}_2]^{(6+3n)+}$ transmitter would affect the kinetic characteristic of the motional correlation. Recently, we have found that monovalent Ag^+ and divalent Hg^{2+} ions, both of which prefer a linear two-coordinate geometry, are hierarchically arranged on the $\mathbf{G^1}$ and $\mathbf{G^2}$ metal binding sites of **1**, respectively, in an electrostatically controlled manner.[19] On the basis of this finding, we have developed a sandwich-shaped $[Ag_6Hg_3\mathbf{1}_2\cdot\mathbf{2}_2]^{12+}$ complex quantitatively formed in solution. In this case, the central three Ag^+ ions on the $\mathbf{G^2}$ ligand sites of the transmitter were expected to be specifically substituted by three Hg^{2+} ions. In fact, ^{1}H NMR and ESI-TOF mass measurements of a mixture of **1**, **2**, AgOTf, and $Hg(OTf)_2$ in a 2:2:6:3 ratio demonstrated the exclusive formation of an alternative RTR, $[Ag_6Hg_3\mathbf{1}_2\cdot\mathbf{2}_2]^{12+}$ complex. The ^{1}H NMR spectrum of the complex at 323 K (Figure 7) displayed resonances for both **1** and **2** with C_3 symmetry as observed with $[Ag_9\mathbf{1}_2\cdot\mathbf{2}_2]^{9+}$. This result suggests the formation of a quadruple-decker $[Ag_6Hg_3\mathbf{1}_2\cdot\mathbf{2}_2]^{12+}$ complex with an identical structural symmetry to that of $[Ag_9\mathbf{1}_2\cdot\mathbf{2}_2]^{9+}$. Moreover, the resonances for the protons of the oxazoline rings $\mathbf{G^2}$, *a* and *b*, for $[Ag_6Hg_3\mathbf{1}_2\cdot\mathbf{2}_2]^{12+}$ shifted to 5.1 and 4.6 ppm, respectively, whose magnitude is greater than $[Ag_9\mathbf{1}_2\cdot\mathbf{2}_2]^{9+}$. On the other hand, the proton signals of ring $\mathbf{G^1}$, *c* and *d*, for $[Ag_6Hg_3\mathbf{1}_2\cdot\mathbf{2}_2]^{12+}$ stayed almost constant as seen with those for $[Ag_9\mathbf{1}_2\cdot\mathbf{2}_2]^{9+}$. This suggests that the divalent Hg^{2+} ions were site-selectively placed on the $\mathbf{G^2}$ ligand rings as expected from our previous study.[19] In addition, the ESI-TOF mass spectrum showed a signal at m/z = 1728.7 assignable to $[Ag_6Hg_3\mathbf{1}_2\cdot\mathbf{2}_2\cdot(OTf)_9]^{3+}$ (Figure S5). These results lead to a conclusion that the three Hg^{2+} ions are bound by the outer rings $\mathbf{G^2}$ of **1** in the center of the $[Ag_6Hg_3\mathbf{1}_2\cdot\mathbf{2}_2]^{12+}$ complex.[20] This heteronuclear complex was also formed by the selective replacement of the three Ag^+ ions in the middle of $[Ag_9\mathbf{1}_2\cdot\mathbf{2}_2]^{9+}$. Upon the addition of 3 equiv of $Hg(OTf)_2$ to a solution of $[Ag_9\mathbf{1}_2\cdot\mathbf{2}_2]^{9+}$, the complex was quickly converted into $[Ag_6Hg_3\mathbf{1}_2\cdot\mathbf{2}_2]^{12+}$ (Figure 8). Then, $[Ag_9\mathbf{1}_2\cdot\mathbf{2}_2]^{9+}$ regenerated as a result of the trapping of the three Hg^{2+} ions from $[Ag_6Hg_3\mathbf{1}_2\cdot\mathbf{2}_2]^{12+}$ by [2,2,2]-cryptand which has a higher affinity to Hg^{2+} than to Ag^+ (Figure 8).[21] Thus, these complexes are interconvertible with each other by addition of Hg^{2+} and [2,2,2]-cryptand one after the other.

The intramolecular ligand exchange in the $[Ag_6Hg_3\mathbf{1}_2\cdot\mathbf{2}_2]^{12+}$ complex was examined by VT ^{1}H NMR study. Proton signals, *g* and *h*, became broadened upon cooling down to 273 K, and then both signals were finally divided into two sets at 243 K (Figure 7). The kinetic parameters for the ligand exchange are

(20) The ^{1}H NMR spectrum of $[Ag_6Hg_3\mathbf{1}_2\cdot\mathbf{3}_2]^{12+}$ complex at 323 K displayed three resonances for protons *a*, *c*, and *d* of **1**, exhibiting the relatively free rotation of the two rotors. VT ^{1}H NMR spectra are shown in Figure S10. The formation of $[Ag_6Hg_3\mathbf{1}_2\cdot\mathbf{3}_2]^{12+}$ was also demonstrated by ESI-TOF mass spectrometry (Figure S6).

(21) Bessiere, J.; Lejaille, M. F. *Anal. Lett.* **1979**, *12*, 753.

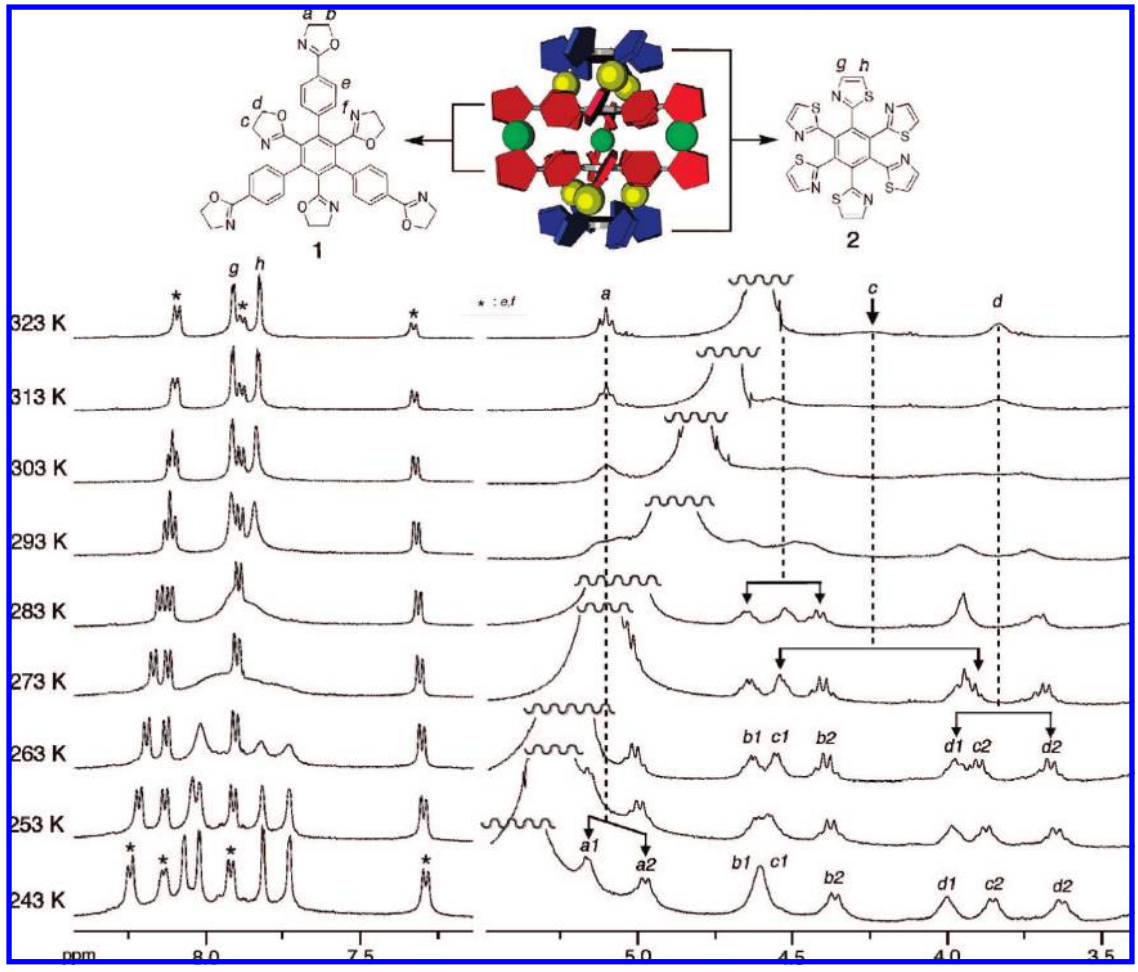

Figure 7. Partial VT ^{1}H NMR spectra (500 MHz, CD_3OD) of a molecular rotor−transmitter−rotor, $Ag_6Hg_3\mathbf{1}_2\cdot\mathbf{2}_2\cdot(OTf)_{12}$. $[Ag_6Hg_3\mathbf{1}_2\cdot\mathbf{2}_2\cdot(OTf)_{12}] = 3.7$ mM.

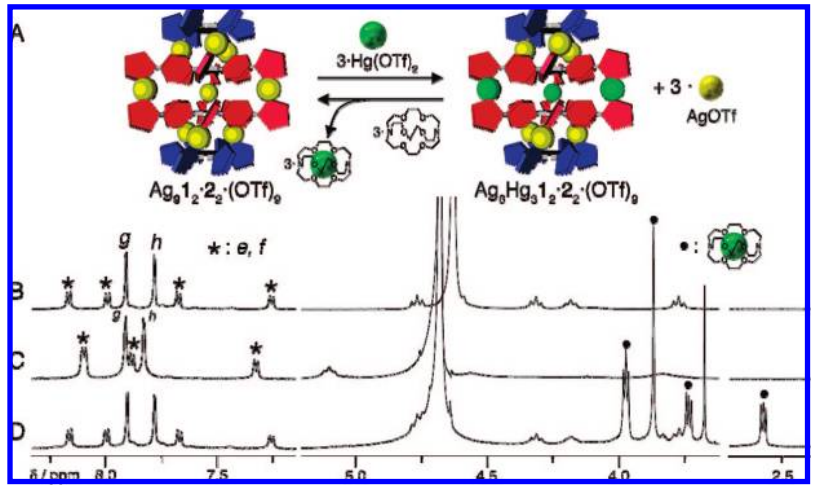

Figure 8. Interconversion between the $Ag_9\mathbf{1}_2\cdot\mathbf{2}_2\cdot(OTf)_9$ and $Ag_6Hg_3\mathbf{1}_2\cdot\mathbf{2}_2\cdot(OTf)_{12}$ complexes. (A) Schematic representation of an interconversion between the $Ag_9\mathbf{1}_2\cdot\mathbf{2}_2\cdot(OTf)_9$ and $Ag_6Hg_3\mathbf{1}_2\cdot\mathbf{2}_2\cdot(OTf)_{12}$ complexes. (B−D) ^{1}H NMR spectra for the replacement of the central three metal ions, $Ag^+\rightarrow Hg^{2+}\rightarrow Ag^+$ (500 MHz, CD_3OD, 313 K, [**1**] = [**2**] = 7.5 mM). (B) $Ag_9\mathbf{1}_2\cdot\mathbf{2}_2\cdot(OTf)_9$. (C) Upon addition of $Hg(OTf)_2$ (3 equiv) to the sample for panel B, $Ag_6Hg_3\mathbf{1}_2\cdot\mathbf{2}_2\cdot(OTf)_{12}$ complex was formed. (D) Upon addition of [2,2,2]-cryptand (3 equiv) to the sample for panel C, $Ag_9\mathbf{1}_2\cdot\mathbf{2}_2\cdot(OTf)_9$ complex was regenerated as a result of the formation of $Hg^{2+}\subset$[2,2,2]-cryptand.

summarized in Table 1. The comparison of smaller $\Delta H^{\ddagger}_{ex}$ and $\Delta S^{\ddagger}_{ex}$ values found for $[Ag_6Hg_3\mathbf{1}_2\cdot\mathbf{2}_2]^{12+}$ with $[Ag_9\mathbf{1}_2\cdot\mathbf{2}_2]^{9+}$ indicates the lesser extent of interlocking between the central two ligands **1** in the $[Ag_6Hg_3\mathbf{1}_2]^{12+}$ transmitter. These results are well explained by the fact that an ionic radius of Hg^{2+} is larger than that of Ag^+. The distance between two ligands **1** in the transmitter $[Ag_6Hg_3\mathbf{1}_2]^{12+}$ should be longer when larger Hg^{2+} ions are placed between them. The structural change would reduce the steric hindrance between the two ligands **1**, which makes the $\Delta H^{\ddagger}_{ex}$ value smaller, and would further relax

the strained structure in the ground state, which results in lowering the $\Delta S^{\ddagger}_{ex}$ value.

Conclusion

In conclusion, we have first developed a molecular rotor–transmitter–rotor (RTR) device, in which the rotational motions of two terminal rotors 1.5 nm apart are strongly correlated through a metal-mediated transmitter. Furthermore, the rate of rotational motions were successfully regulated by changing the kind of metal ions in the transmitter. The single-crystal X-ray analysis of $Ag_9\mathbf{1}_2\cdot\mathbf{2}_2\cdot(OTf)_9$ revealed that the two terminal rotors **2** are coaxially stacked through the transmitter, and that they have an identical helicity. Large entropy changes of both the intramolecular ligand exchange and the helix inversion were found in the RTR devices, $[Ag_6M_3\mathbf{1}_2\cdot\mathbf{2}_2]^{(6+3n)+}$ ($M^{n+} = Ag^+$ or Hg^{2+}), whereas $[Ag_3\mathbf{2}\cdot\mathbf{5}]^{3+}$, which is a part of the RTR, showed a negative entropy change. In addition, the helix inversions of all the rings in the device take place with comparable rate constants. Taken all together, we conclude that the rotational motions of the remotely stacked rotors are highly correlated with each other through the oscillating transmitter. The mechanism of motion has two elements, the ligand exchange and the flip motion, both of which accompany a simultaneous, oscillating motion between *P* and *M* helical isomers of the two rotors and the transmitter put between them.[22] The helix inversion of a transmitter would be a highly controllable mode for a long-range transmission of motions, because the change in helicity on one side of the transmitter could propagate efficiently to the other side along the rotational axis of the transmitter consisting of simple repeating units.[23] Therefore, the propagation distance of the motions between two rotors would be easily altered by the number of repeating units in the transmitter. In our $[Ag_6M_3\mathbf{1}_2]^{(6+3n)+}$ transmitters, for example, the insertion of a predetermined number of disk-shaped ligands in the transmitters with the aid of metal-coordination would form a multilayered transmitter to realize a longer-range transmission of motions. Toward more complex molecular machine systems, one can connect a variety of motor and actuator molecules to the transmitter mediated by a terminal rotor containing an anchoring functional group such as molecule **3**. Such a strategy would be widely applicable to transmission of motions within a molecular machine system fitted with artificial molecular devices or natural macromolecules, for example, motor proteins.

Experimental Section

All ambient and variable-temperature ^{1}H NMR spectra were recorded on a Bruker DRX 500 (500 MHz) spectrometer using TMS as the internal reference. Electrospray ionization-time-of-flight (ESI-TOF) mass spectra were recorded on a Micromass LCT mass spectrometer KB 201. High-resolution mass spectra of $[Ag_9\mathbf{1}_2\cdot\mathbf{2}_2]^{9+}$ and $[Ag_6Hg_3\mathbf{1}_2\cdot\mathbf{2}_2]^{12+}$ complexes were recorded on a QFT-7 (IonSpec FTMS Systems, Varian Inc.) mass spectrometer. Intensity data for X-ray crystallographic analysis were obtained on a Rigaku RAXIS-RAPID Imaging Plate diffractometer with graphite monochromated Cu Kα radiation.

Preparation of Molecular RTRs. $Ag_9\mathbf{1}_2\cdot\mathbf{2}_2\cdot(OTf)_9$ complex: To a solution of **1** (2.2 mg, 3.0 μmol) in CD_3OD, **2** (1.7 mg, 3.0 μmol) was suspended, and then a CD_3OD solution of AgOTf (51 μL of 0.26 M solution, 13.4 μmol) was added. The mixture was allowed to stand at room temperature for a few minutes. ^{1}H NMR spectra for the titration studies demonstrated the formation of the $Ag_9\mathbf{1}_2\cdot\mathbf{2}_2\cdot(OTf)_9$ complex as shown in Figure S1. ^{1}H NMR (500 MHz, CD_3OD, 313 K) δ 8.17 (dd, J = 8.1, 1.2 Hz, 6H), 8.00 (dd, J = 8.1, 1.2 Hz, 6H), 7.91 (d, J = 3.4 Hz, 12 H), 7.79 (d, J = 3.2 Hz, 12H), 7.68 (d, J = 7.8 Hz, 6H), 7.26 (d, J = 7.8 Hz, 6H), 4.77 (t, J = 9.7 Hz, 12H), 4.32 (t, J = 9.5 Hz, 12H), 4.19 (t, J = 9.2 Hz, 12H), 3.78 (t, J = 9.7 Hz, 12H). ESI-TOF mass (positive) *m*/*z* 2304.5 $[Ag_9\mathbf{1}_2\cdot\mathbf{2}_2\cdot(OTf)_7]^{2+}$, 1487.1 $[Ag_9\mathbf{1}_2\cdot\mathbf{2}_2\cdot(OTf)_6]^{3+}$. HRMS (ESI) *m*/*z*: exact mass $[Ag_9\mathbf{1}_2\cdot\mathbf{2}_2(OTf)_6]^{3+}$ 1486.7638, $C_{138}H_{96}Ag_9N_{24}O_{30}S_{18}$, requires 1486.7618.

$Ag_9\mathbf{1}_2\cdot\mathbf{3}_2\cdot(OTf)_9$ complex: To a solution of **1** (2.3 mg, 3.2 μmol) and **3** (1.9 mg, 3.2 μmol) in CD_3OD, a CD_3OD solution of AgOTf (36 μL of 0.39 M solution, 14.2 μmol) was added. The mixture was allowed to stand at room temperature for a few minutes. ^{1}H NMR titration studies demonstrated the formation of the $Ag_9\mathbf{1}_2\cdot\mathbf{3}_2\cdot(OTf)_9$ complex as shown in Figure S2. ^{1}H NMR (500 MHz, CD_3OD, 303 K) δ 8.16 (dd, J = 8.1, 1.2 Hz, 6H), 7.99 (dd, J = 7.8, 1.5 Hz, 3H), 7.93 (d, J = 3.2 Hz, 4H), 7.92 (d, J = 3.4 Hz, 2H), 7.90 (d, J = 3.4 Hz, 4H), 7.79 (d, J = 3.7 Hz, 4H), 7.78 (d, J = 3.7 Hz, 4H), 7.77 (d, J = 3.2 Hz, 2H), 7.67 (dd, J = 7.8, 1.5 Hz, 3H), 7.64 (s, 2H), 7.25 (dd, J = 8.1, 1.5 Hz, 3H), 4.32 (t, J = 9.7 Hz, 12H), 4.18 (br, 12 H), 3.77 (t, J = 9.3 Hz, 12H). ESI-TOF mass (positive) *m*/*z* 1507.5 $[Ag_9\mathbf{1}_2\cdot\mathbf{3}'_2\cdot(OTf)_6]^{3+}$, in which **3′** denotes the deuterated form of hydroxy groups of **3**.

$Ag_6Hg_3\mathbf{1}_2\cdot\mathbf{2}_2(OTf)_{12}$ complex: To a solution of **1** (2.1 mg, 2.9 μmol) in CD_3OD (0.4 mL), **2** (1.7 mg, 2.9 μmol) in CD_3OD (0.4 mL) was suspended, and then a CD_3OD solution of $Hg(OTf)_2$ (22 μL of 0.2 M solution, 4.4 μmol) and a CD_3OD solution of AgOTf (19 μL of 0.46 M solution, 8.8 μmol) were added. The mixture was allowed to stand at room temperature for a few minutes. Its ^{1}H NMR spectrum showed the quantitative formation of $Ag_6Hg_3\mathbf{1}_2\cdot\mathbf{2}_2(OTf)_{12}$ complex. ^{1}H NMR (500 MHz, CD_3OD, 313 K) δ 8.10 (d, J = 8.1 Hz, 12 H), 7.92 (d, J = 3.2 Hz, 12H), 7.89 (d, J = 7.8 Hz, 6H), 7.83 (d, J = 2.9 Hz, 12H), 7.33 (d, J = 8.1 Hz, 6H), 5.1 (t, J = 9.7 Hz, 12H), 4.56 (br, 12H), 3.84 (br, 12H). ESI-TOF mass (positive) *m*/*z* 1728.7 $[Ag_6Hg_3\mathbf{1}_2\cdot\mathbf{2}_2(OTf)_9]^{3+}$. HRMS (ESI) *m*/*z*: exact mass $[Ag_6Hg_3\mathbf{1}_2\cdot\mathbf{2}_2(OTf)_9]^{3+}$ 1728.4446, $C_{141}H_{96}Ag_6Hg_3N_{24}O_{39}S_{21}$, requires 1728.4449.

Crystal data for $Ag_9\mathbf{1}_2\cdot\mathbf{2}_2\cdot(OTf)_9\cdot(CH_3OH)_7$: $C_{148}H_{100}Ag_9F_{27}N_{24}O_{46}S_{21}$, M = 5107.58, T = 93.1 K, triclinic, $P\bar{1}$, Z = 2, a = 21.2194(9), b = 21.3055(8), c = 24.4632(19) Å, α = 89.325(3), β = 79.310(3), γ = 63.263(3)°, V = 9673.3(7) Å^3, 56643 measured reflections, 32928 unique reflections, R = 0.1345, wR = 0.3904, GOF = 1.054. Material details for the crystal structure are available free of charge from the Cambridge Crystallographic Data Centre under deposition number CCDC 627131.

$Ag_6Hg_3\mathbf{1}_2\cdot\mathbf{3}_2(OTf)_{12}$ complex: To a solution of **1** (2.1 mg, 2.9 μmol) and **3** (1.7 mg, 2.9 μmol) in CD_3OD (0.4 mL), a CD_3OD solution of $Hg(OTf)_2$ (21 μL of 0.2 M solution, 4.3 μmol) and a CD_3OD solution of AgOTf (18.5 μL of 0.46 M solution, 8.6 μmol) were added. The mixture was allowed to stand at room temperature for a few minutes. ^{1}H NMR (500 MHz, CD_3OD, 313 K) δ 8.11 (d, J = 6.9 Hz, 6H), 8.09 (d, J = 7.1 Hz, 6H), 7.94−7.77 (m, 26H), 7.33 (d, J = 7.6 Hz, 6H), 5.11 (t, J = 8.3 Hz, 12H), 4.57 (br, 12H), 3.83 (br, 12H). ESI-TOF mass (positive) *m*/*z* 1748.8 $[Ag_6Hg_3\mathbf{1}_2\cdot\mathbf{3}'_2(OTf)_9]^{3+}$, in which **3′** denotes the deuterated form of hydroxy groups of **3**.

Preparation of $[Ag_3\mathbf{2}\cdot\mathbf{5}]^{3+}$ Complex. To a solution of **2** (2.3 mg, 3.9 μmol) and **5** (2.0 mg, 3.9 μmol) in CD_3OD (0.55 mL) was added a solution of AgOTf (3.0 mg, 11.7 μmol), and then the mixture was allowed to stand at room temperature for a few minutes. Variable-temperature ^{1}H NMR spectra are shown in Figure S11. ^{1}H NMR (500 MHz, CD_3OD, 293 K) δ 7.89 (d, J = 8.5 Hz, 3H), 7.88 (d, J = 3.5 Hz, 6H), 7.75 (d, J = 3.5 Hz, 6H), 7.57−7.55

(22) In this study the synchronous helix inversions were demonstrated for the RTRs. Since the helix inversion takes place both by the ligand exchange (EX) and the flip motion (flip), if both motions take place at the same frequency, every co-occurring combination of the ligand exchange and the flip motion on both sides, that is, EX(rotor A)−EX(rotor B), EX(rotor A)−flip(rotor B), flip(rotor A)−EX(rotor B), or flip(rotor A)−flip(rotor B) is possible. In the present case, the detailed information is missing on this point.

(23) Pijper, D.; Feringa, B. L. *Angew. Chem., Int. Ed.* **2007**, *46*, 3693.

(m, 6H), 7.33−7.31 (m, 3H), 7.26−7.22 (m, 3H), 4.03 (t, $J = 9.8$ Hz, 6H), 3.68 (t, $J = 9.8$ Hz, 6H); ESI-TOF mass (positive) $m/z =$ 781.4 $[Ag_3\mathbf{2}\cdot\mathbf{5}\cdot(OTf)]^{2+}$, 471.3 $[Ag_3\mathbf{2}\cdot\mathbf{5}]^{3+}$.

Analysis of the Ligand Exchange in Molecular RTR Devices. The kinetic parameters for the ligand exchange of the RTR devices and molecular ball bearing, $[Ag_3\mathbf{2}\cdot\mathbf{5}]^{3+}$, are summarized in Table 1. The rate constant at each temperature was estimated from the line shape analysis for thiazolyl proton signals of **2**, and $\Delta H^{\ddagger}$ and $\Delta S^{\ddagger}$ values were determined by Eyring plot. Simulated spectra and Eyring plots are shown in Figures S11−S13.

Acknowledgment. We thank A. Sato of JASCO International Co., LTD. for measuring the high-resolution FT mass spectra of the metal complexes. This work was supported by Grants-in-Aid for Scientific Research (S) to M.S. (No. 16105001) and Young Scientists (A) to S.H. (No. 17685005) from the Ministry of Education, Culture, Sports, Science and Technology of Japan, CASIO science promotion foundation, and Inamori foundation.

Supporting Information Available: Synthetic procedures, VT ^{1}H NMR spectra, ESI-TOF mass spectra. This material is available free of charge via the Internet at http://pubs.acs.org.

JA8014583